Improved Interpolated Correction Schemes for Dual-Level Direct Dynamics Calculation

Chun-Huei Huang, Ru-Min You, Pei-Yin Lian, and Wei-Ping Hu*

Department of Chemistry, National Chung Cheng University Chia-Yi, Taiwan 621

Received: April 3, 2000; In Final Form: June 1, 2000

A set of new correction schemes for dual-level variational transition-state theory calculation has been developed. In the new schemes, an intermediate level of theory is employed to better estimate the width of the reaction energy barrier. Then, adjustable parameters are set in the final calculation to reproduce the estimated high-level barrier width in addition to the high-level energy of reaction and barrier height. The new schemes have been tested in the rate constant calculation of $H + H_2S \rightarrow HS + H_2$ and $OH + CH_4 \rightarrow H_2O + CH_3$ reactions with potential energy surface information obtained from several low- and high-level ab initio theories. Compared to the previous correction schemes, the dual-level calculation based on the new schemes produced results, in most cases, in significantly better agreement with the reference high-level calculation. The new schemes are expected to predict more accurate rate constants for those reactions in which tunneling effects are important.

1. Introduction

Reaction dynamics calculation is usually sensitive to some local and global features of the potential energy surface (PES). The sensitivity to the PES information greatly limits the ability to perform accurate dynamics calculation for larger chemical systems since accurate PES data, especially those about the global features, are usually prohibitively difficult to obtain. Variational transition-state theory[1,2] (VTST) shows that one only needs information on the most important regions of the PES to calculate the reaction rate constants. In the most commonly used VTST approaches, the regions include primarily the reaction path[1−3] and, if tunneling calculation is desired, the assumed tunneling paths.[2,4,5] The VTST thus enables one to calculate the rate constants of more complex reactions by reducing the required global PES data. This is particularly true in the direct dynamics[5−7] approach, where the PES information is calculated on the fly instead of being obtained from a fitted analytical function.

However, even with the VTST approach, accurately calculating the reaction path of a polyatomic system is still a formidable task in most cases. Using lower-level ab initio theory or semiempirical methods to calculate the PES data reduces the necessary computational resources but usually at the expense of the accuracy of the calculation. In recent years, dual-level (DL) dynamics[8−11] approaches for VTST calculation have been developed to partially resolve the accuracy versus affordability dilemma. In a typical dual-level VTST calculation, the entire reaction-path information (geometry, energies, gradients, vibrations, etc.) is calculated at a qualitatively correct level of electronic structure theory, while the properties of the most important points on the reaction path, usually the reactants, saddle point, and products (and sometimes the reaction complexes) are calculated at the highest affordable theoretical level or are obtained from available experimental data. Then, the low-level (LL) to high-level (HL) correction along the reaction path is applied using interpolated correction schemes based on the corrections at the stationary points that are calculated at the high level. This type of dual-level approaches has been applied to the study of many chemical systems[8−10,12−14] and has yielded good agreement with available experimental data.[8,9,13]

Several interpolated correction schemes have been critically evaluated recently,[11] and the original SECKART method has stood the test. On the other hand, the current correction schemes only guarantee that, in using the dual-level approaches, the high-level transition-state theory (TST)[1] rate constants are reproduced since only the high-level stationary point properties are used. One cannot, however, fine-tune the performance of the dual-level calculation to the variational and tunneling effects since they are determined by more global features of the PES which are more difficult for the correction schemes to handle properly with the high-level information only at stationary points. In the current study, we propose three new interpolated correction schemes based on the original SECKART scheme.[8] These new schemes involve an additional "intermediate level" (IL) of calculation to estimate the width of the high-level energy barrier along the reaction path. The interpolated correction schemes are then constrained to reproduce the estimated barrier width. Since the tunneling effects are usually sensitive to the barrier width, the new correction schemes are expected to be more accurate in predicting the rate constants when tunneling effects are important. We used the hydrogen abstraction reactions of

$$H + H_2S \rightarrow HS + H_2 \qquad \text{(R1)}$$

$$OH + CH_4 \rightarrow H_2O + CH_3 \qquad \text{(R2)}$$

as our test cases. We performed full VTST calculation including tunneling corrections using PES data obtained from a "higher" and several "lower" levels of electronic structure theory for each reaction. We tested our new correction schemes against currently available schemes on how well the lower-level calculation could be made (by applying various dual-level correction schemes) to reproduce the results from the higher-level calculation using only the higher-level stationary point information.

2. Methodology

We first give a short review of the currently available dual-level correction schemes. When the high-level calculation

* E-mail: chewph@ccunix.ccu.edu.tw. Fax: 886-5-272-1040.

10.1021/jp001273j CCC: $19.00
Published on Web 07/18/2000

involves both the geometry optimization and frequency calculation of the stationary points, as proposed in the original dual-level procedures,[8] the dual-level correction is denoted as IOC (interpolated optimized correction).[11] The original SECKART scheme[8] corrects the low-level classical energy (or Born−Oppenheimer energy) profile (relative to the reactants) along the reaction path of a bimolecular reaction by

$$V_{\mathrm{MEP,DL}}(s) = V_{\mathrm{MEP,LL}}(s) + E_{\mathrm{S}}(s;L) \tag{1}$$

where s is the mass-scaled reaction coordinate and $E_{\mathrm{S}}(s;L)$ is an Eckart correction function whose values at reactants ($s = -\infty$), saddle point ($s = 0$), and products ($s = \infty$) are determined by the low- to high-level corrections at these three points. The "width" of the Eckart function is determined by the range parameter L, which is determined by the half-width of the low-level $V_{\mathrm{MEP}}(s)$. (Similar correction methods are also used for the correction of vibrational frequencies.[8,10]) One of the underlying assumption of the SECKART scheme is that the shapes, or more precisely, the barrier widths, calculated at the high and low levels are similar. However, depending on the selection of the high and low levels, the assumption is not always valid.

An alternative approach, which is now called the DECKART scheme, has been used for the study of the reaction of hydrogen atom with *trans*-N_2H_2.[10] In the DECKART scheme, an Eckart function is used to fit the high-level classical energy profile along the reaction path based on the stationary point energies of the reactants, the transition state, and the products, and the imaginary frequency calculated at the high-level transition state. Another Eckart function is used to fit the low-level classical energy profile along the reaction path based on the stationary point energies and the low-level barrier width. (The original SECKART scheme also includes this step, but the fit is discarded once the range parameter L is determined.) The correction function is then defined as the difference between the two Eckart functions:

$$E_{\mathrm{D}}(s) = \mathrm{Eckart}_{\mathrm{HL}}(s) - \mathrm{Eckart}_{\mathrm{LL}}(s) \tag{2}$$

and the dual-level corrected $V_{\mathrm{MEP}}(s)$ is obtained by

$$V_{\mathrm{MEP,DL}}(s) = V_{\mathrm{MEP,LL}}(s) + E_{\mathrm{D}}(s) \tag{3}$$

Encouraging results were obtained for the H + *trans*-N_2H_2 system using the DECKART scheme. However, it was later recognized that the DECKART scheme did not always provide successful dual-level correction.[11]

Two other interpolated schemes, IOE (interpolated optimized energy) and ISPE (interpolated single-point energy), have also been proposed and tested in a recent article.[11] The IOE scheme, which is a simpler version of IOC, omits the calculation of frequencies at the high level. In the ISPE scheme, high-level single-point energy evaluation is performed at a series of selected points along the low-level reaction path. Interpolated correction for the energies is then applied based on the correction at the selected points in the dual-level dynamics calculation. The vibrational frequencies are not corrected in either schemes. The IOE scheme performed moderately well, but the omission of frequency correction may lead to larger errors at high temperatures. While the ISPE scheme incorporates correction to barrier-width, the inaccurate reaction energy barrier and vibrational frequencies may lead to even larger errors. After a critical evaluation, the authors of the article concluded that the IOC procedure with the SECKART scheme gave the best overall performance.

In the current study, we seek to develop improved correction schemes that incorporate the correction to geometry, energies, frequencies, and barrier width in a more consistent fashion. While the geometry optimization and frequency calculation at the higher level are important, a reasonable and systematic way of correcting the width of the energy barrier is of crucial importance for accurate dynamics calculation including tunneling. Our new correction schemes are based on the original SECKART interpolation scheme, and as the energy profile along the reaction path is corrected, results calculated at an additional intermediate level (IL) of theory are also taken into account.

When tunneling effects are important, it is desirable to obtain the barrier width as accurately as possible. However, in the original SECKART scheme, the dual-level corrected barrier width is largely determined by the low-level calculation. If the topology of the low-level PES is qualitatively different from that of the high level, significant errors will occur in the tunneling calculation even though the PES data at the stationary points are corrected. To calibrate the dual-level correction on the barrier width, one has to know the energy of at least one extra point, preferably not very close to the transition state, on the high-level reaction path in addition to the stationary points. For example, one may wish to have the dual-level corrected V_{MEP} or vibrationally adiabatic ground-state (V_a^G) energy curve along the reaction path to coincide with their high-level values at the half-height width of the classical energy barrier at the reactant (product) side in an exoergic (endoergic) reaction. That is

$$V_{\mathrm{MEP,DL}}(s_{1/2}) = V_{\mathrm{MEP,HL}}(s_{1/2}) \tag{4}$$

or

$$V_a^{\mathrm{G}}{}_{\mathrm{DL}}(s_{1/2}) = V_a^{\mathrm{G}}{}_{\mathrm{HL}}(s_{1/2}) \tag{5}$$

The $s_{1/2}$ is defined by

$$V_{\mathrm{MEP,HL}}(s_{1/2}) = {}^1/_2 \Delta V^{\neq}_{\mathrm{HL}} \tag{6}$$

where $\Delta V^{\neq}_{\mathrm{HL}}$ is the high-level classical energy barrier, and by definition

$$V_a^{\mathrm{G}}{}_{\mathrm{HL}}(s_{1/2}) = V_{\mathrm{MEP,HL}}(s_{1/2}) + \mathrm{ZPE}^{\mathrm{GT}}{}_{\mathrm{HL}}(s_{1/2}) \tag{7}$$

where $\mathrm{ZPE}^{\mathrm{GT}}$ denotes the vibrational zero-point energy of the generalized transition states.[1,2] The difficulty lies in the fact that $s_{1/2}$ and $V_a^{\mathrm{G}}{}_{\mathrm{HL}}(s_{1/2})$ are difficult to determine accurately since the high-level reaction path is not calculated (usually because the calculation is too resource demanding). However, our past experience and the current study led us to believe that a calibration to the barrier width, although difficult, is essential to obtain consistent and accurate results in tunneling calculation. As mentioned above, in the original SECKART scheme, the range parameter L is determined by the low-level V_{MEP}. However, if the high-level reaction path information can be estimated, it is possible to adjust the range parameter to satisfy eqs 4 or 5. In the present study, we propose three levels of correction schemes to incorporate the IOC−SECKART scheme with calculation at an intermediate level (IL) of theory for the classical energy along the reaction path. (The vibrational frequencies are not calculated at this level; thus this is much less resource demanding than a full reaction-path free-energy calculation.) In all schemes, the reaction coordinate $s_{1/2}$ is obtained at the intermediate level of theory to approximate the half-height width of the high-level classical barrier. That is, the

$s_{1/2}$ is approximated by finding the reaction coordinate in the intermediate-level calculation to satisfy:

$$V_{\mathrm{MEP,IL}}(s_{1/2}) = {}^1/_2\Delta V^{\neq}_{\mathrm{IL}} \tag{8}$$

where $\Delta V^{\neq}_{\mathrm{IL}}$ is the classical barrier height calculated at the intermediate level of theory. The rest of this section assumes an exoergic bimolecular reaction in which $s_{1/2}$ is negative. The expressions for an endoergic reaction can be obtained by replacing "reactant" to "product" and $s_{1/2}$ to the corresponding positive value.

The SIL-1 Scheme. This scheme involves adjusting the range parameter L of the Eckart correction function in a dual-level dynamics calculation to reproduce half of the high-level classical energy barrier at the estimated location of $s_{1/2}$ on the reactant side of the reaction path. That is,

$$V_{\mathrm{MEP,DL}}(s_{1/2};L) = {}^1/_2\Delta V^{\neq}_{\mathrm{HL}} \tag{9}$$

where $\Delta V^{\neq}_{\mathrm{HL}}$, the high-level barrier height, is obtained by either ab initio calculation or fitting to experimental data. The advantage of this scheme over the original SECKART method is that if the shape of V_{MEP} of the low level is markedly different from that of the high level, an estimate of the high-level barrier width using an appropriate intermediate level of calculation should make the dual-level correction much more reliable. In the current study, the sole purpose of the intermediate-level calculation is to obtain the $s_{1/2}$ in eq 8. Once the $s_{1/2}$ has been determined, the range parameter L is determined through eq 1 by the condition of eq 9. The range parameter thus determined is then used in the subsequent dual-level rate constant calculation.[8]

The SIL-2 Scheme. The vibrationally adiabatic ground-state energy curve $V_a^G(s)$ is the effective potential energy barrier in the zero- and small-curvature tunneling (ZCT and SCT) approximations.[2,5a,15] Thus, instead of fitting the dual-level V_{MEP} at $s_{1/2}$, we seek to fit the dual-level $V_a^G(s)$ at $s = s_{1/2}$ to an estimated high-level value in this scheme. This involves approximating the last term of eq 7 since the reaction-path calculation is not performed at the high level. In this scheme the following approximation is used:

$$\mathrm{ZPE}^{\mathrm{GT}}{}_{\mathrm{HL}}(s_{1/2}) \approx \mathrm{ZPE}^{\mathrm{GT}}{}_{\mathrm{LL}}(s_{1/2}) + {}^1/_2\Delta \tag{10}$$

where Δ is defined as

$$\Delta = [\mathrm{ZPE}^{\ddagger}{}_{\mathrm{HL}} - \mathrm{ZPE}^{\ddagger}{}_{\mathrm{LL}}] + [\mathrm{ZPE}^{\mathrm{R}}{}_{\mathrm{HL}} - \mathrm{ZPE}^{\mathrm{R}}{}_{\mathrm{LL}}] \tag{11}$$

where $\mathrm{ZPE}^{\ddagger}$ and $\mathrm{ZPE}^{\mathrm{R}}$ are the vibrational zero-point energies of the transition state and the reactants, respectively. That is, the high-level $\mathrm{ZPE}^{\mathrm{GT}}(s_{1/2})$ is approximated as the sum of the low-level $\mathrm{ZPE}^{\mathrm{GT}}(s_{1/2})$ and a correction term. The correction term is defined as the average of the low- to high-level zero-point energy corrections at the transition state and at the reactants. This approximation is justified by the fact that $\mathrm{ZPE}^{\mathrm{GT}}(s)$ along the reaction path calculated at the low level should give the correct trend of the zero-point energy changes. Furthermore, the ${}^1/_2\Delta$ correction term is generally small and should be in the right direction. Then, similar to the SIL-1 scheme, the range parameter L is determined by the condition:

$$V_a^{\mathrm{G}}{}_{\mathrm{DL}}(s_{1/2};L) = {}^1/_2\Delta V^{\neq}_{\mathrm{HL}} + \mathrm{ZPE}^{\mathrm{GT}}{}_{\mathrm{HL}}(s_{1/2}) \tag{12}$$

with the understanding that the last term in eq 12 is approximated by eqs 10 and 11. The range parameter thus determined is then used in the subsequent dual-level rate constant calculation. Since the current scheme fits the dual-level adiabatic ground-state energy curve (V_a^G) to the estimated high-level value at $s_{1/2}$, the dual-level V_{MEP} curve obtained in this scheme is in general different from that obtained in the SIL-1 scheme where the V_{MEP} curve is fitted directly. It is also noted that in schemes SIL-1 and SIL-2 a single range parameter is used for both the classical energy and vibrational frequency correction.

The SIL-3 Scheme. In the original SECKART scheme, the range parameters for the energy and frequency correction are arbitrarily set to the same value. With the inclusion of the intermediate-level calculation, it is also possible to fit both the dual-level $V_{\mathrm{MEP}}(s)$ and $V_a^G(s)$ at $s_{1/2}$ to the estimated high-level values. Thus, we propose here another scheme that uses two different range parameters L_1 and L_2 to satisfy both the conditions of eqs 9 and 12. That is, L_1 is determined by eq 9 *first*, and then the frequency correction is based on a different range parameter L_2 in order to satisfy eq 12.

Choices for the Intermediate Level. Although it seems that the intermediate level should be as close to the high level as possible, one should be aware that a qualitatively correct low level is also important for a successful dual-level calculation, as will be seen in the next section. It is thus not recommended to put all of the available computational resources in the high- and intermediate-level calculation and only use a low-quality calculation to obtain the underlying PES information. Furthermore, the molecular geometry along the reaction path is not directly corrected. Implicit correction for the geometry is made by multiplying the low-level determinant of moment of inertia by a scaling factor that is determined at the saddle point.[8] However, some of the related properties, such as the normal-mode eigenvectors and the gradient vectors along the reaction path are not corrected. Thus a quality low-level calculation is also essential for accurate dual-level dynamics calculation.

The SIL schemes proposed above do *not* restrict the levels of theory used for the intermediate-level calculation. However, an obvious and convenient choice is to perform a double-slash (//) calculation on the reaction-path geometry calculated at the low level, provided that the low-level calculation gives reasonable reaction-path geometry. This is similar to the ISPE approach[11] except that the level for energy calculation (the level before the // sign) is not necessarily the same as the high level. One also should be aware that the intermediate-level energy profile thus obtained might not have its maximum value at the low-level transition-state geometry. For consistency, shifting of the reaction coordinates in the calculated $V_{\mathrm{MEP,IL}}(s)$ is performed before assigning $s_{1/2}$ in eq 8.

3. Computational Details

To test the performance of the new correction schemes, we carried out full VTST with semiclassical tunneling calculation using PES information calculated at higher levels of ab initio theory to represent the "high-level" or the reference results. We also calculated the full reaction-path information at various lower levels of theory to serve as the "low-level" data. Classical energies along the reaction path are also calculated at the levels of theory intermediate of the low and high levels. Different correction schemes are then applied to the low-level data based on the stationary point information and on the intermediate-level classical energy profiles along the reaction path. The calculated reaction rate constants are then compared to the reference values calculated at the high level to determine the accuracy of different interpolated correction schemes. Comparison with experimental values is *not* the focus of this work.

The "high-level" ab initio theory used is Møller−Plesset second-order perturbation theory[16,17] with the 6-31+G** basis set[18] (MP2/6-31+G**) for R1, and MP2 with the correlation-consistent valence double-ζ basis set[18] (MP2/cc-pVDZ) for R2. The "low-level" ab initio theories used include MNDO,[19] Hartree−Fock method[16] with the 3-21+G* basis set (HF/3-21+G*), MP2/3-21+G*, and HF/6-31+G** for R1, and MP2/3-21+G, MP2/6-31G** for R2. The intermediate levels employed in the current study are the double-slash method (high level) // (low level) except for R1 with MNDO low-level theory where the MP2/6-31+G**//HF/3-21+G* level was also used as the intermediate-level calculation. Cubic polynomial fits are used to determine the values of $s_{1/2}$ from the intermediate-level classical energy profile. The ICL method[8,10] is used in correcting the vibrational frequencies. In a few cases, range parameters simultaneously satisfy eqs 9 and 12 (SIL-3) cannot be found, and only the dual-level corrections based on SIL-1 and SIL-2 schemes are performed.

The rate constants are calculated at eight temperatures (200, 250, 300, 400, 500, 600, 800, and 1000 K) and at the levels of conventional transition-state theory (TST), canonical variational theory (CVT),[1,2] canonical variational theory with small-curvature tunneling approximation (CVT/SCT), and canonical variational theory with large-curvature tunneling approximation (CVT/LCT)[2,4,5b,15] including only the vibrational ground-state product. Another popular tunneling correction method, the microcanonical optimized multidimensional tunneling (μOMT) approximation,[5b] which takes the dominant tunneling probability between the SCT and LCT methods at any given energies, is not used here. This is because the individual SCT and LCT calculations would give clearer tests on how well the new schemes can reproduce the high-level results when the two different tunneling approximations are used.

In the VTST calculation, the scaled mass is set to 1 amu, and the harmonic approximation is used for vibration in all calculation. The redundant internal coordinate system[20] is used in the vibrational analysis of the generalized transition states. For R1, the reaction path is calculated using the Page−McIver algorithm[21] from −1.4 to +0.8 bohrs with gradient and Hessian step sizes of 0.005 and 0.025 bohrs, respectively. For R2, the reaction path is also calculated using the Page−McIver algorithm from −3.0 to +0.6 bohrs with gradient and Hessian step sizes of 0.005 and 0.025 bohrs, respectively. In all of the dual-level large-curvature tunneling calculations, the linear correction method[8] for potential energy is used in the nonadiabatic region.[4,5b,15] That is, the correction for the potential energies in the straight-line tunneling path within the nonadiabatic region is obtained using a linear correction function of the mass-scaled distance to one of the termini of the path, regardless of the relative magnitude of the corrections at the termini and at the saddle point. The coefficients of this function are found by the classical energy corrections at the termini, which in turn are determined by the classical energy correction function along the reaction path. Detailed implementation can be found elsewhere.[4,8] We found (data not shown) this method to be more consistent in reproducing the high-level results while the quadratic correction method originally proposed[8] was found to be less reliable in the current study.

The electronic structure calculation on the stationary points was performed using the *Gaussian 98* program.[18] The dual-level direct dynamics calculation was carried out using the *Gaussrate* 8.2 program,[22] which provides an interface between *Gaussian 98* and a locally modified *Polyrate* 8.2 program.[23]

TABLE 1: Calculated Born−Oppenheimer Energies of Reaction and Barrier Heights[a] of R1 at Various Levels

	E_{rxn}	$\Delta V^{\neq}$
MNDO	−18.13	5.23
HF/3-21+G*	−15.98	12.06
HF/6-31+G**	−16.63	12.31
MP2/3-21+G*	−11.86	10.60
MP2/6-31+G*//MNDO	−11.67	10.02
MP2/6-31+G**// HF/3-21+G*	−13.83	8.85
MP2/6-31+G**// HF/6-31+G**	−13.80	8.79
MP2/6-31+G*//MP2/3-21+G*	−13.80	8.71
MP2/6-31+G**	−13.79	8.69
QCISD(T)/6-311+G(3df,2dp)[b]	−14.93	4.44
expt.	−16.40[c] (−14.95)[d]	

[a] In kilocalorie per mole. [b] From Peng et al.[24] and recalculated in this work. [c] From Chase et al.[25] and using the calculated zero-point and thermal energies at QCISD(T)/6-311+G(3df,2dp) level. [d] From Nicovich[26] and using the calculated zero-point and thermal energies at QCISD(T)/6-311+G(3df,2dp) level.

TABLE 2: Calculated Rate Constants[a] of R1 at the High-Level (MP2/6-31+G)**

T(K)	TST	CVT	CVT/SCT	CVT/LCT
200	6.14(−20)[b]	5.79(−20)	6.98(−17)	4.96(−17)
250	3.59(−18)	3.43(−18)	3.33(−16)	2.36(−16)
300	5.46(−17)	5.27(−17)	1.30(−15)	8.31(−16)
400	1.71(−15)	1.67(−15)	1.04(−14)	6.40(−15)
500	1.43(−14)	1.40(−14)	4.55(−14)	3.05(−14)
600	6.13(−14)	6.06(−14)	1.38(−13)	1.00(−13)
800	4.18(−13)	4.15(−13)	6.61(−13)	5.42(−13)
1000	1.45(−12)	1.44(−12)	1.94(−12)	1.70(−12)

[a] In cubic centimeters per molecule per second. [b] 6.14(−20) means 6.14×10^{-20}.

4. Results and Discussion

(1) $H + H_2S \rightarrow HS + H_2$. The reaction energies and classical barrier heights calculated at the high, intermediate, and low levels are listed in Table 1. Values from a previous calculation[24] and from experiments[25,26] are also included for comparison. The calculated geometry and frequencies of the stationary points are included in the Supporting Information. The semiempirical methods have been popular choices for the low-level calculation because of their low computational cost. However, the semi-empirical methods sometimes give very different transition-state geometry than that from high-level ab initio calculation. For the current reaction, only the MNDO method provides reasonable transition-state geometry, and thus it is the only semi-empirical method used for the low-level calculation. Table 2 shows the calculated rate constants at the single high level (MP2/6-31+G**). These rate constants are used as the standard to evaluate the quality of different dual-level correction schemes. Tables 3−5 compare the calculated dual-level rate constants using the MNDO low level and various correction schemes to the high-level values. (Results using two different intermediate levels are included.) Tables 6−8, 9−11, and 12−14 show similar comparison using HF/3-21+G*, MP2/3-21+G*, and HF/6-31+G** as the low levels of theory, respectively.

In Table 1, we see that, except for the MNDO level, all other low-level energies of reaction are in reasonable agreement with the high-level (MP2/6-31+G**) value. The low-level energy barriers are different from the high-level value by 2.4−3.6 kcal/mol. All of the energies of reaction and the energy barriers calculated at intermediate levels agree well with the high-level calculation. As expected, the results involving MNDO calculation show the largest errors. It can be seen from Table 2 that in the high-level calculation there are little variational effects (difference between the TST and CVT rate constants) but there

TABLE 3: Ratios of the Calculated Dual-Level CVT Rate Constants to the High-Level Values (k_{DL}/k_{HL}) of R1 Using Different Correction Schemes with the MNDO Low Level

T (K)	DECKART	SECKART	SIL-1	SIL-2
200	0.93	0.74	0.80[a] (0.84)[b]	0.79 (0.82)
250	0.95	0.80	0.85 (0.87)	0.83 (0.86)
300	0.96	0.84	0.88 (0.90)	0.79 (0.86)
400	0.98	0.90	0.93 (0.94)	0.92 (0.93)
500	0.99	0.93	0.95 (0.96)	0.81 (0.96)
600	0.99	0.95	0.96 (0.97)	0.96 (0.97)
800	0.99	0.97	0.98 (0.99)	0.98 (0.98)
1000	0.99	0.97	0.99 (0.99)	0.99 (0.99)
av[c]	1.03	1.14	1.09 (1.07)	1.14 (1.09)

[a] Numbers without parentheses are results using MP2/6-31+G**// MNDO as the intermediate level. [b] Numbers in parentheses are results using MP2/6-31+G**//HF/3-21+G* as the intermediate level. [c] Defined as the average of 10^x, $x = |\log(k_{DL}/k_{HL})|$, over the eight temperatures. It is thus defined to avoid unequal weighting on overestimation and underestimation of the rate constants.

TABLE 4: Ratios of the Calculated Dual-Level CVT/SCT Rate Constants to the High-Level Values (k_{DL}/k_{HL}) of R1 Using Different Correction Schemes with the MNDO Low Level

T (K)	DECKART	SECKART	SIL-1	SIL-2
200	134.71	0.10	1.19 (2.28)	1.06 (1.56)
250	54.52	0.20	1.19 (2.11)	0.88 (1.51)
300	25.05	0.30	1.13 (1.82)	0.85 (1.37)
400	8.63	0.49	1.06 (1.48)	0.87 (1.21)
500	4.60	0.62	1.03 (1.31)	0.90 (1.13)
600	3.09	0.71	1.01 (1.21)	0.92 (1.09)
800	1.98	0.81	1.00 (1.11)	0.95 (1.04)
1000	1.58	0.87	0.99 (1.07)	0.96 (1.02)
av[a]	29.27	3.19	1.08 (1.55)	1.10 (1.24)

[a] See footnotes below Table 3.

TABLE 5: Ratios of the Calculated Dual-Level CVT/LCT Rate Constants to the High-Level Values (k_{DL}/k_{HL}) of R1 Using Different Correction Schemes with the MNDO Low Level

T (K)	DECKART	SECKART	SIL-1	SIL-2
200	49.80	0.05	0.58 (1.09)	0.37 (0.76)
250	18.73	0.11	0.57 (0.97)	0.39 (0.71)
300	9.40	0.22	0.63 (0.97)	0.49 (0.75)
400	3.78	0.48	0.79 (1.01)	0.69 (0.87)
500	2.28	0.66	0.88 (1.02)	0.81 (0.93)
600	1.74	0.76	0.92 (1.02)	0.87 (0.96)
800	1.34	0.86	0.95 (1.00)	0.92 (0.97)
1000	1.18	0.90	0.96 (1.00)	0.95 (0.98)
av[a]	11.03	4.96	1.33 (1.02)	1.66 (1.17)

[a] See footnotes below Table 3.

are significant tunneling effects. For example, inclusion of small-curvature tunneling results in approximately 1200 and 25 times increases in the CVT rate constants at 200 and 300 K, respectively. The small-curvature tunneling is slightly more important than the large-curvature tunneling in the calculation.

Table 3 shows that the high-level CVT rate constants are well reproduced by all of the correction schemes, which is expected since there are little variational effects. In Tables 4 and 5, we find that the DECKART scheme severely overestimates the tunneling effects. The original SECKART scheme performs better; however, it significantly underestimates the tunneling and is less satisfactory than the new SIL-1 and SIL-2 schemes. The improvement by the new correction schemes can be visualized and understood in Figure 1 where the $V_a^G(s)$ curves calculated at the high, low, and dual levels with the DECKART, the original SECKART, and the new SIL-2 schemes, respectively, are plotted. It is clearly shown that the DECKART scheme predicts a barrier that is too narrow, and the original SECKART predicts a barrier that is too wide. This is why the DECKART scheme overestimates the tunneling effects whereas the SECKART scheme underestimates the tunneling effects. The SIL-2 scheme predicts a $V_a^G(s)$ curve very similar to that of the high level. Suitable range parameters cannot be found to perform the SIL-3 correction scheme. Using the reaction-path geometry calculated at a slightly higher level in the intermediate-level calculation only results in noticeable improvement in the large-curvature tunneling calculation.

When the HF/3-21+G* calculation is used as the low-level theory, all of the correction schemes accurately reproduce the

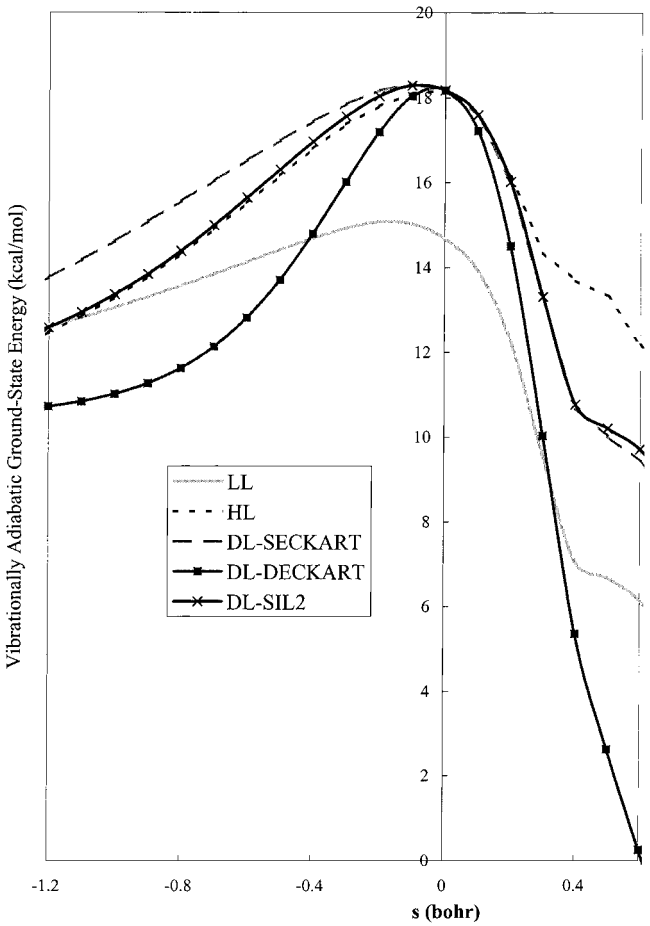

Figure 1. Calculated vibrationally adiabatic ground-state energy curve along the reaction path [$V_a^G(s)$] at the MNDO low level (LL), the MP2/6-31+G** high level (HL), dual-level with the SECKART scheme (DL-SECKART), dual-level with the DECKART scheme (DL-SECKART), and dual-level with the SIL-2 scheme (DL-SIL-2) using the MP2/6-31+G**//MNDO intermediate level.

TABLE 6: Ratios of the Calculated Dual-Level CVT/SCT Rate Constants to the High-Level Values (k_{DL}/k_{HL}) of R1 Using Different Correction Schemes with the HF/3-21+G* Low Level

T (K)	DECKART	SECKART	SIL-1	SIL-2	SIL-3
200	10.24	1.48	0.66	0.73	0.72
250	6.70	1.48	0.81	0.88	0.87
300	4.64	1.42	0.89	0.95	0.95
400	2.79	1.29	0.97	1.01	1.00
500	2.06	1.21	1.00	1.02	1.02
600	1.69	1.15	1.00	1.02	1.02
800	1.37	1.09	1.01	1.02	1.02
1000	1.23	1.06	1.01	1.01	1.01
av[a]	3.84	1.27	1.11	1.08	1.08

[a] See footnotes below Table 3.

TABLE 7: Ratios of the Calculated Dual-Level CVT/LCT Rate Constants to the High-Level Values (k_{DL}/k_{HL})of R1 Using Different Correction Schemes with the HF/3-21+G* Low Level

T (K)	DECKART	SECKART	SIL-1	SIL-2	SIL-3
200	6.53	1.00	0.41	0.47	0.42
250	4.75	1.21	0.64	0.70	0.65
300	3.68	1.34	0.85	0.91	0.87
400	2.48	1.38	1.08	1.12	1.10
500	1.89	1.30	1.12	1.15	1.13
600	1.60	1.24	1.12	1.13	1.13
800	1.31	1.14	1.08	1.08	1.08
1000	1.19	1.09	1.05	1.06	1.05
av[a]	2.93	1.21	1.33	1.27	1.32

[a] See footnotes below Table 3.

TABLE 8: Ratios of the Calculated Dual-Level CVT/SCT Rate Constants to the High-Level Values (k_{DL}/k_{HL}) of R1 Using Different Correction Schemes with the MP2/3-21+G* Low Level

T (K)	DECKART	SECKART	SIL-1	SIL-2
200	10.70	3.52	0.72	0.78
250	7.90	2.63	0.80	0.87
300	5.05	2.05	0.87	0.92
400	2.78	1.51	0.94	0.98
500	1.98	1.30	0.97	1.00
600	1.62	1.19	0.98	1.00
800	1.31	1.10	0.99	1.00
1000	1.19	1.06	0.99	1.01
av[a]	4.07	1.79	1.11	1.07

[a] See footnotes below Table 3.

TABLE 9: Ratios of the Calculated Dual-Level CVT/LCT Rate Constants to the High-Level Values (k_{DL}/k_{HL})of R1 Using Different Correction Schemes with the MP2/3-21+G* Low Level

T (K)	DECKART	SECKART	SIL-1	SIL-2
200	27.82	13.37	1.49	1.56
250	13.98	7.92	1.40	1.48
300	8.06	5.23	1.40	1.48
400	3.58	2.77	1.35	1.40
500	2.23	1.87	1.26	1.29
600	1.72	1.52	1.20	1.22
800	1.34	1.24	1.11	1.12
1000	1.20	1.14	1.07	1.08
av	7.49	4.38	1.28	1.33

TABLE 10: Ratios of the Calculated Dual-Level CVT/SCT Rate Constants to the High-Level Values (k_{DL}/k_{HL}) of R1 Using Different Correction Schemes with the HF/6-31+G Low Level**

T (K)	DECKART	SECKART	SIL-1	SIL-2	SIL-3
200	9.63	0.91	0.63	0.70	0.69
250	6.52	1.02	0.78	0.84	0.84
300	4.62	1.06	0.87	0.92	0.92
400	2.81	1.08	0.95	0.98	0.98
500	2.07	1.07	0.98	1.01	1.01
600	1.70	1.06	0.99	1.01	1.01
800	1.38	1.04	1.00	1.01	1.01
1000	1.23	1.03	1.01	1.01	1.01
av[a]	3.74	1.06	1.14	1.09	1.10

[a] See footnotes below Table 3.

high-level CVT rate constants within 6% (data not shown). Tables 6 and 7 show that the DECKART scheme again overestimates the tunneling effects, and all three new schemes performed slightly better than the original SECKART scheme in the SCT calculation. All of the SECKART based schemes performed equally well for the LCT calculation. In comparing

TABLE 11: Ratios of the Calculated Dual-Level CVT/LCT Rate Constants to the High-Level Values (k_{DL}/k_{HL}) of R1 Using Different Correction Schemes with the HF/6-31+G Low Level**

T (K)	DECKART	SECKART	SIL-1	SIL-2	SIL-3
200	6.05	0.65	0.42	0.49	0.44
250	4.66	0.85	0.63	0.70	0.65
300	3.71	1.01	0.82	0.89	0.85
400	2.52	1.16	1.04	1.09	1.06
500	1.90	1.17	1.09	1.12	1.11
600	1.60	1.15	1.10	1.11	1.11
800	1.31	1.09	1.07	1.08	1.07
1000	1.19	1.06	1.05	1.05	1.05
av[a]	2.87	1.17	1.32	1.25	1.30

[a] See footnotes below Table 3.

TABLE 12: Calculated Born−Oppenheimer Energies of Reaction and Barrier Heights[a] of R2 at Various Levels

	E_{rxn}	$\Delta V^{\neq}$
MP2/3-21+G	−4.74	13.28
MP2/6-31G**	−9.90	12.16
MP2/cc-pVDZ//MP2/3-21+G	−8.33	11.76
MP2/cc-pVDZ//MP2/6-31G**	−10.18	10.44
MP2/cc-pVDZ	−10.22	10.46
MP−SAC2//MP2/adj-cc-pVTZ[b]	−13.27	7.37

[a] In kilocalorie per mole. [b] From Melissas and Truhlar.[27]

TABLE 13: Calculated Rate Constants[a] of R2 at the High-Level (MP2/cc-pVDZ)

T (K)	TST	CVT	CVT/SCT	CVT/LCT
200	6.80 (−21)[b]	2.44 (−22)	3.02 (−20)	4.73 (−20)
250	5.92 (−19)	3.69 (−20)	7.28 (−19)	6.06 (−19)
300	1.21 (−17)	1.08 (−18)	8.53 (−18)	5.90 (−18)
400	5.87 (−16)	8.08 (−17)	2.63 (−16)	1.86 (−16)
500	6.75 (−15)	1.17 (−15)	2.52 (−15)	1.95 (−15)
600	3.76 (−14)	7.48 (−15)	1.28 (−14)	1.05 (−14)
800	3.84 (−13)	8.67 (−14)	1.17 (−13)	1.04 (−13)
1000	1.81 (−12)	4.26 (−13)	5.14 (−13)	4.75 (−13)

[a] In cubic centimeters per molecule per second. [b] 6.80(−21) means 6.80×10^{-21}.

TABLE 14: Ratios of the Calculated Dual-Level CVT Rate Constants to the High-Level Values (k_{DL}/k_{HL}) of R2 Using Different Correction Schemes with the MP2/3-21+G Low Level

T (K)	DECKART	SECKART	SIL-1	SIL-2
200	26.30	12.11	7.54	3.01
250	15.38	8.55	5.81	2.72
300	10.81	6.79	4.88	2.54
400	7.09	5.08	3.92	2.34
500	5.65	4.24	3.43	2.21
600	4.95	3.74	3.11	2.13
800	4.37	3.18	2.74	2.01
1000	4.20	2.86	2.54	1.93
av	9.84	5.82	4.25	2.36

Tables 3−5, we find that using a better low-level ab initio theory, on average, gives better results by all of the correction schemes.

When the MP2/3-21+G* calculation is used as the low-level theory, high-level CVT rate constants again are well reproduced by all correction schemes (within 5%, data not shown). Tables 8 and 9 show that both the SIL-1 and SIL-2 schemes perform much better than the DECKART and original SECKART schemes when tunneling effects are considered in the calculation. Suitable range parameters cannot be found for the SIL-3 correction scheme.

When the HF/6-31+G** calculation is used as the low-level theory, the calculated CVT rate constants are within 5% of the

TABLE 15: Ratios of the Calculated Dual-Level CVT/SCT Rate Constants to the High-Level Values (k_{DL}/k_{HL}) of R2 Using Different Correction Schemes with the MP2/3-21+G Low Level

T (K)	DECKART	SECKART	SIL-1	SIL-2
200	8509.93	2.97	1.45	0.53
250	1744.51	3.85	2.23	0.94
300	481.83	3.99	2.58	1.23
400	77.19	3.75	2.75	1.55
500	32.70	3.50	2.73	1.70
600	17.89	3.27	2.66	1.76
800	9.40	2.96	2.53	1.81
1000	5.04	2.74	2.41	1.81
av[a]	1359.81	3.38	2.28	1.60

[a] See footnotes below Table 3.

TABLE 16: Ratios of the Calculated Dual-Level CVT/LCT Rate Constants to the High-Level Values (k_{DL}/k_{HL}) of R2 Using Different Correction Schemes with the MP2/3-21+G Low Level

T (K)	DECKART	SECKART	SIL-1	SIL-2
200	8773.96	4.39	2.39	1.10
250	2930.92	6.66	3.98	1.80
300	846.37	6.68	4.39	2.12
400	118.69	5.32	3.95	2.20
500	35.55	4.41	3.49	2.15
600	17.33	3.86	3.18	2.09
800	8.53	3.25	2.80	2.00
1000	6.35	2.92	2.58	1.93
av	1592.21	4.68	3.34	1.92

high-level values by all correction schemes (data not shown). As seen in Tables 10 and 11, the results using SECKART and the three new schemes are all very similar. (The SECKART scheme performed better at lower temperatures whereas the new schemes performed better at higher temperatures. However, the differences are small.) This is understandable by the fact that when the quality of low-level theory approaches that of the high-level theory, results from all of the SECKART-based methods should converge. This is not true for the DECKART scheme, as seen in Tables 10 and 11, where it still significantly overestimates the tunneling effects.

Overall, the SIL-1 and SIL-2 schemes performed equally well, and they are less sensitive to the low-level theory used than the DECKART and original SECKART schemes. No consistent improvement is obtained with the additional effort spent in the SIL-3 scheme. As seen in Tables 5, 7, 9, and 11, the reasonable agreement between the high-level and dual-level CVT/LCT results (30% error on average) using the new schemes is especially encouraging since the energy correction in the nonadiabatic region is very difficult. For R1, Table 2 shows that the small-curvature tunneling seems to be the dominant tunneling mechanism. Since the new correction schemes give very good results both on SCT and LCT calculation, it is anticipated that they will give better μOMT results than those of the DECKART and the original SECKART schemes in cases when the SCT and LCT are equally important.[5b,9]

(2) $OH + CH_4 \rightarrow H_2O + CH_3$. The reaction energies and classical barrier heights calculated at the high, intermediate, and low levels are listed in Table 12. Values from a previous study[27] are also listed. The calculated geometry and frequencies of the stationary points are included in the Supporting Information. Table 13 shows the calculated rate constants at the single high level (MP2/cc-pVDZ). These rate constants are again used as the standard to evaluate the quality of different dual-level correction schemes. Tables 14−16 compare the calculated dual-level rate constants using MP2/3-21+G low level and various

TABLE 17: Ratios of the Calculated Dual-Level CVT Rate Constants to the High-Level Values (k_{DL}/k_{HL}) of R2 Using Different Correction Schemes with the MP2/6-31G Low Level**

T (K)	DECKART	SECKART	SIL-1	SIL-2	SIL-3
200	21.06	1.19	1.16	1.13	1.10
250	12.45	1.16	1.13	1.10	1.08
300	8.79	1.13	1.11	1.09	1.06
400	5.74	1.10	1.08	1.06	1.05
500	4.50	1.07	1.07	1.05	1.03
600	3.77	1.06	1.05	1.04	1.02
800	2.81	1.04	1.03	1.02	1.01
1000	2.37	1.02	1.02	1.01	1.00
av	7.69	1.10	1.08	1.06	1.04

TABLE 18: Ratios of the Calculated Dual-Level CVT/SCT Rate Constants to the High-Level Values (k_{DL}/k_{HL}) of R2 Using Different Correction Schemes with the MP2/6-31G Low Level**

T (K)	DECKART	SECKART	SIL-1	SIL-2	SIL-3
200	9411.14	0.77	0.65	0.56	0.56
250	1621.88	0.91	0.82	0.74	0.74
300	413.68	0.98	0.91	0.84	0.84
400	70.08	1.03	0.98	0.93	0.92
500	24.97	1.03	1.00	0.97	0.96
600	10.09	1.03	1.01	0.98	0.97
800	4.75	1.02	1.01	0.99	0.97
1000	3.19	1.01	1.00	0.99	0.98
av[a]	1444.97	1.07	1.11	1.19	1.19

[a] See footnotes below Table 3.

TABLE 19: Ratios of the Calculated Dual-Level CVT/LCT Rate Constants to the High-Level Values (k_{DL}/k_{HL}) of R2 Using Different Correction Schemes with the MP2/6-31G Low Level**

T (K)	DECKART	SECKART	SIL-1	SIL-2	SIL-3
200	7995.94	0.60	0.49	0.41	0.41
250	2393.33	0.90	0.79	0.70	0.69
300	650.78	1.04	0.95	0.88	0.87
400	84.28	1.08	1.04	1.00	0.98
500	23.57	1.08	1.05	1.02	1.01
600	8.42	1.06	1.05	1.02	1.01
800	3.77	1.04	1.03	1.02	1.00
1000	2.61	1.03	1.02	1.01	0.99
av[a]	1395.34	1.14	1.19	1.26	1.26

[a] See footnotes below Table 3.

correction schemes to the high-level values. Tables 17−19 show the same comparison using MP2/6-31G** calculation as the low level of theory.

As reported in a recent article,[28] it is relatively difficult to obtain reasonable energy of reaction using lower-level ab initio calculation for R2. Thus the choices of the low-level calculation are more limited. As seen in Table 12, the low-level energy barriers are different from the high-level value by 1.7−2.8 kcal/mol. All of the energies of reaction and the barrier heights calculated at the intermediate levels agree well with the high-level calculation. In contrast to R1, Table 13 shows that there are very large variational effects in the high-level calculation. For example, at 300 K the variational effects lower the TST rate constant by over an order of magnitude. The large variational effects provide a severe challenge to the dual-level dynamics calculation. The two low-level theories used here represent two different extremes. The MP2/3-21+G calculation represents a low-quality source of PES information, and it predicts variational effects very different than those predicted by the high-level calculation. The MP2/6-31G** calculation represents a high-quality source of PES information, and it predicts variational effects similar to those by the high-level

calculation. As also seen in Table 13, the tunneling effects are very important at lower temperatures. The small-curvature tunneling is more important except at the lowest temperature.

As seen in Table 14, when the MP2/3-21+G is used as the low-level calculation, significant errors in CVT are obtained using all correction schemes, with the largest errors from the DECKART scheme and the smallest from the SIL-2 scheme. The errors are less severe for the SECKART-based schemes when the tunneling effects are included, as seen in Tables 15 and 16. The SIL-2 is significantly better than other dual-level correction schemes. Most of the errors are due to the much smaller variational effects predicted by the low-level theory. (The rate constants calculated at the single low level are listed in the Supporting Information.)

When the MP2/6-31G** calculation is used as the low-level theory, all correction schemes, except for DECKART, accurately reproduce the high-level CVT rate constants, as seen in Table 17. Tables 18 and 19 show that all four SECKART-based schemes produce very similar CVT/SCT and CVT/LCT rate constants, and they are all in good agreement with the high-level values in Table 13. (Again, the SECKART scheme performed slightly better at lower temperatures while the new SIL schemes performed slightly better at higher temperatures.) This clearly illustrates that when the variational effects are important, a quality low-level PES is required to obtain accurate reaction rate constants using the dual-level dynamics methods.

5. Applicability and Concluding Remarks

The original SECKART scheme can easily be applied to most bimolecular reactions with almost any combinations of the low- and high-level theory. The most serious drawback of the original SECKART scheme, however, is that the dual-level corrected barrier width is largely determined by the low-level PES, which might not be reliable. The new SIL correction schemes include an additional intermediate-level calculation to estimate the high-level barrier width. By adjusting the range parameters, one can make the dual-level corrected barrier width as close to the estimated high-level value as possible. However, the applicability of the new schemes is somewhat more limited by the way the dual-level correction is applied. For example, if both the low- and high-level calculation predict approximately the same classical barrier height, only very small correction can be made to the low-level $V_{MEP}(s)$ from the reactants to the transition state by the SECKART-based schemes. It is then possible that no appropriate range parameters can be found to satisfy eq 9 or 12. A detailed study of the SECKART correction scheme shows that when

$$\Delta V^{\ddagger}_{LL} - \Delta V^{\ddagger}_{HL} > 0 \tag{13}$$

and

$$\Delta V^{\ddagger}_{LL} - \Delta V^{\ddagger}_{HL} > V_{MEP,LL}(s_{1/2}) - {}^{1}/_{2}\Delta V^{\ddagger}_{HL} > 0 \tag{14}$$

or when

$$\Delta V^{\ddagger}_{HL} - \Delta V^{\ddagger}_{LL} > 0 \tag{15}$$

and

$$\Delta V^{\ddagger}_{HL} - \Delta V^{\ddagger}_{LL} > {}^{1}/_{2}\Delta V^{\ddagger}_{HL} - V_{MEP,LL}(s_{1/2}) > 0 \tag{16}$$

an appropriate range parameter L can be found to satisfy eq 9; that is, the SIL-1 scheme can be applied. When a lower-level ab initio calculation is used as the low-level theory, eq 13 is usually satisfied since the high-level barrier is normally a few kilocalorie per mole lower than that of the low level. Furthermore, when the barrier difference is not very small, eq 14 is usually automatically satisfied. There are cases in which the high-level barriers are higher than the low-level values (eq 15). As long as the difference is not too small, eq 16 is also satisfied most of the time. When eq 14 or 16 is not satisfied, it is usually an indication that the low-level theory used is not appropriate.

TABLE 20: Average Errors[a] by Different Correction Schemes

	DECKART	SECKART	SIL-1	SIL-2	SIL-3
R1[b]	8.15	2.38	1.23	1.23	1.20
R2	968.31	2.87	2.21	1.57	1.16

[a] See text and footnotes below Table 3. [b] The errors of CVT rate constants are not included because there are only very small variational effects in R1.

Experience also showed that when the difference in eq 13 or 15 is as large as a few kilocalorie per mole, an appropriate range parameter can easily be found to satisfy eq 12, and thus the SIL-2 scheme can be applied. For the SIL-3 scheme, the dual-level corrected zero-point energies along the reaction path are usually much less sensitive to the range parameter (L_2) used for the frequency correction. If the zero-point energy changes from the reactants to the transition state are very different in the low- and high-level calculations, the range parameters L_2 may not be found, as shown in the previous section. From the above discussion, when one wishes to apply the new SIL schemes, the barrier height predicted by the low-level theory usually has to be at least a few kilocalorie per mole different from the high-level value. It is a *different* notion from that in some of previous studies.[8,10,11] For the energy of reaction, good agreement with the high-level value is still recommended in choosing the low-level theory. Table 20 shows the average errors of different correction schemes considered in the current study by averaging the last rows of Tables 4−11 and Tables 14−19 for R1 and R2, respectively. The new SIL schemes are significantly better than the DECKART and SECKART schemes. Although the SIL-3 scheme seems to give the lowest errors, its applicability is much more limited as discussed above.

The large variational effects in R2 calculated at the MP2/cc-pVDZ and MP2/6-31G** levels raise concerns on the accuracy of the previous calculation[8,27] that did not show significant variational effects. Further study at higher-levels of theory might be necessary to resolve the discrepancy, which in turn, may resolve the discrepancy[27−29] in the calculated barrier heights of R2 by different groups. (That is, larger variational effects would favor a lower barrier height when the experimental rate constants are modeled.)

6. Summary

We have developed three new correction schemes for dual-level VTST direct dynamics calculation. The new schemes are based on the original SECKART method with inclusion of an additional intermediate-level calculation to better estimate the width of the reaction energy barrier. We have tested the new schemes against the original SECKART and DECKART schemes on two hydrogen abstraction reactions by comparing the dual-level corrected results using various low levels of theory to the results of a single high-level calculation. In most cases, the new schemes out-performed the original SECKART scheme when tunneling effects were considered. When a high-quality low-level theory was used, all SECKART-based methods performed equally well. In real application for larger systems,

however, using a very high-quality calculation as the low-level theory might not be computationally tractable. Thus, the new correction schemes, in particular, the SIL-2 scheme, are recommended over the original SECKART scheme. The current study also illustrated that when the variational effects are important, the choice of a qualitatively correct low-level theory is of crucial importance for accurate modeling of the reaction rate constants.

Acknowledgment. This work is supported in part by the National Science Council of Taiwan, Republic of China, Grant Number NSC 89-2113-M-194-006. The authors are grateful to Prof. Donald G. Truhlar of the University of Minnesota for providing the *Gaussrate* interface program.

Supporting Information Available: Tables of calculated stationary point geometry and vibrational frequencies, low-level rate constants, $s_{1/2}$ values from intermediate-level calculation, and range parameters used for dual-level calculation. This material is available free of charge via the Internet at http://pubs.acs.org.

References and Notes

(1) Truhlar, D. G.; Garrett, B. C. *Acc. Chem. Res.* **1980**, *13*, 440.
(2) Truhlar, D. G.; Isaacson, A. D.; Garrett, B. C. In *Theory of Chemical Reaction Dynamics*; Baer M., Ed.; CRC Press: Boca Raton, FL, 1985; Vol. 4, p 65.
(3) Truhlar, D. G. In *The Reaction Path in Chemistry*; Heidrich, D., Ed.; Kluwer: Dordrecht, 1995; p 229.
(4) Garrett, B. C.; Joseph, T.; Truong, T. N.; Truhlar, D. G. *Chemi. Phys.* **1989**, *136*, 271.
(5) (a) Liu, Y.-P.; Lynch, G. C.; Truong, T. N.; Lu, D.-h.; Truhlar, D. G.; Garrett, B. C. *J. Am. Chem. Soc.* **1993**, *115*, 2408. (b) Liu, Y.-P.; Lu, D.-h.; Gonzalez-LaFont, A.; Truhlar, D. G. *J. Am. Chem. Soc.* **1993**, *115*, 7806.
(6) Truhlar D. G.; Garrett, B. C.; Klippenstein, S. J. *J. Phys. Chem.* **1996**, *100*, 12771.
(7) (a) Gonzalez-LaFont, A.; Truong, T. N.; Truhlar, D. G. *J. Phys. Chem.* **1991**, *95*, 4618. (b) Storer, J. W.; Houk, K. N. *J. Am. Chem. Soc.* **1993**, *115*, 10426.
(8) Hu, W.-P.; Liu, Y.-P.; Truhlar, D. G. *J. Chem. Soc., Faraday Trans.* **1994**, *90*, 1715.
(9) Corchado, J. C.; Espinosa-Garcia, J.; Hu, W.-P.; Rossi, I.; Truhlar, D. G. *J. Phys. Chem.* **1995**, *99*, 687.
(10) Chuang, Y.-Y.; Truhlar, D. G. *J. Phys. Chem. A* **1997**, *101*, 3808.
(11) Chuang, Y.-Y.; Corchado, J. C.; Truhlar, D. G. *J. Phys. Chem. A* **1999**, *103*, 1140.
(12) Hu, W.-P.; Truhlar, D. G. *J. Am. Chem. Soc.* **1996**, *118*, 860.
(13) Hu, W.-P.; Rossi, I.; Corchado, J. C.; Truhlar, D. G. *J. Phys. Chem. A* **1997**, *101*, 6911.
(14) Hu, W.-P.; Wu, Y.-R. *J. Am. Chem. Soc.* **1999**, *121*, 10168.
(15) Lu, D.-h.; Truong, T. N.; Melissas, V. S.; Lynch, G. C.; Liu, Y.-P.; Garrett, B. C.; Steckler, R.; Isaacson, A. D.; Rai, S. N.; Hancock, G. C.; Lauderdale, J. G.; Joseph, T.; Truhlar, D. G. *Comput. Phys. Commun.* **1992**, *71*, 235.
(16) Hehre, W. J.; Radom, L.; Schleyer, P. v. R.; Pople, J. A. *Ab initio Molecular Orbital Theory*: John Wiley & Sons: New York, 1986.
(17) Møller, C.; Plesset, M. S. *Phys. Rev.* **1934**, *46*, 618.
(18) Frisch, M. J.; Trucks, G. W.; Schlegel, H. B.; Scuseria, G. E.; Robb, M. A.; Cheeseman, J. R.; Zakrzewski, V. G.; Montgomery, J. A., Jr.; Stratmann, R. E.; Burant, J. C.; Dapprich, S. J.; Millam, M.; Daniels, A. D.; Kudin, K. N.; Strain, M. C.; Farkas, O.; Tomasi, J.; Barone, V.; Cossi, M.; Cammi, R.; Mennucci, B.; Pomelli, C.; Adamo, C.; Clifford, S.; Ochterski, J.; Petersson, G. A.; Ayala, P. Y.; Cui, Q.; Morokuma, K.; Malick, D. K.; Rabuck, A. D.; Raghavachari, K.; Foresman, J. B.; Cioslowski, J.; Ortiz, J. V.; Baboul, A. G.; Stefanov, B. B.; Liu, G.; Liashenko, A.; Piskorz, P.; Komaromi, I.; Gomperts, R.; Martin, R. L.; Fox, D. J.; Keith, T.; Al-Laham, M. A.; Peng, C. Y.; Nanayakkara, A.; Gonzalez, C.; Challacombe, M.; Gill, P. M. W.; Johnson, B.; Chen, W.; Wong, M. W.; Andres, J. L.; Gonzalez, C.; Head-Gordon, M.; Replogle, E. S.; Pople, J. A. *Gaussian 98*, rev. A.7; Gaussian, Inc.: Pittsburgh, PA, 1998.
(19) Dewar, M. J. S.; Thiel, W. *J. Am. Chem. Soc.* **1977**, *99*, 4899.
(20) Chuang, Y.-Y.; Truhlar, D. G. *J. Phys. Chem. A* **1998**, *102*, 242.
(21) (a) Page, M.; McIver, J. W., Jr. *J. Chem. Phys.* **1988**, *88*, 922. (b) Page, M.; Doubleday: C.; McIver, J. W., Jr. *J. Chem. Phys.* **1990**, *93*, 5634.
(22) Corchado, J. C.; Chunag, Y.-Y.; Coitino, E. L., Truhlar, D. G. *Gaussrate*, ver. 8.2; University of Minnesota, 1999.
(23) Chunag, Y.-Y.; Corchado, J. C.; Fast, P. L.; Villa, J.; Hu, W.-P.; Liu, Y.-P.; Lynch, G. C.; Nguyen, K. A.; Jackels, C. F.; Gu, M. Z.; Rossi, I.; Coitino, E. L.; Clayton, S.; Melissas, V. S.; Steckler, R.; Garrett, B. C.; Isaacson, A. D.; Truhlar, D. G. *Polyrate*, ver. 8.2; University of Minnesota, 1999.
(24) Peng, J.; Hu, X.; Marshall, P. *J. Phys. Chem. A.* **1999**, *103*, 5307
(25) Chase, M. W., Jr.; Davies, C. A.; Downey, J. R., Jr.; Frurip, D. J.; McDonald, R. A.; Syverud, A. N. *J. Phys. Chem. Ref. Data* **1985**, *14* (Suppl. 1).
(26) Nicovich, J. M.; Kreutter, K. D.; van Dijk, C. A.; Wine, P. H. *J. Phys. Chem.* **1992**, *96*, 2518.
(27) Melissas, V. S.; Truhlar, D. G. *J. Chem. Phys.* **1993**, *99*, 3542.
(28) Chunag, Y.-Y.; Coitino, E. L.; Truhlar, D. G. *J. Phys. Chem. A* **2000**, *104*, 446.
(29) Malick, D. K.; Peterson, G. A. *J. Chem. Phys.* **1998**, *108*, 5704.